Four-dimensional multiphoton imaging of brain entry, amyloid binding, and clearance of an amyloid-β ligand in transgenic mice

Brian J. Bacskai*†, Gregory A. Hickey*, Jesse Skoch*, Stephen T. Kajdasz*, Yanming Wang‡, Guo-feng Huang‡, Chester A. Mathis‡, William E. Klunk‡, and Bradley T. Hyman*

*Department of Neurology/Alzheimer's Disease Research Laboratory, Massachusetts General Hospital, 114 16th Street, Charlestown, MA 02129; and ‡Departments of Psychiatry and Radiology, University of Pittsburgh School of Medicine, Pittsburgh, PA 15213

Edited by L. L. Iversen, University of Oxford, Oxford, United Kingdom, and approved August 13, 2003 (received for review July 2, 2003)

The lack of a specific biomarker makes preclinical diagnosis of Alzheimer's disease (AD) impossible, and it precludes assessment of therapies aimed at preventing or reversing the course of the disease. The development of a tool that enables direct, quantitative detection of the amyloid-β deposits found in the disease would provide an excellent biomarker. This article demonstrates the real-time biodistribution kinetics of an imaging agent in transgenic mouse models of AD. Using multiphoton microscopy, Pittsburgh compound B (PIB) was imaged with sub-μm resolution in the brains of living transgenic mice during peripheral administration. PIB entered the brain quickly and labeled amyloid deposits within minutes. The nonspecific binding was cleared rapidly, whereas specific labeling was prolonged. WT mice showed rapid brain entry and clearance of PIB without any binding. These results demonstrate that the compound PIB has the properties required for a good amyloid-imaging agent in humans with or at risk for AD.

positron emission tomography | senile plaques | Alzheimer's disease

The development of radioligands for *in vivo* imaging in the brain demands the demonstration of specificity for the target with good brain entry and exit kinetics. A technique that would allow direct assessment of the biodistribution kinetics with ligand-receptor specificity simultaneously would hasten development of new radioligands and confirm the utility of existing agents. Multiphoton microscopy is an *in vivo* imaging technique with very high spatial and temporal resolution that allows the precise determination of ligand binding specificity with sub-μm resolution that can be used to characterize imaging probes in small animal models. In the context of Alzheimer's disease (AD), the "receptors" are amyloid-β plaques and neurofibrillary tangles (1, 2). AD is only diagnosed with certainty after death. The definitive diagnosis of this disease in living patients will depend on the detection of one or both of these neuropathological lesions either directly, by means of brain imaging, or indirectly, through a suitable biomarker that parallels their development (3). Progress with therapeutics aimed at removing these lesions will also be accelerated with the use of an end point to evaluate their efficacy (4). Significant progress has been achieved in developing imaging agents that enter the brain and target plaques and tangles specifically to allow direct imaging in humans (5–9). One promising compound, 2-(4′-methylaminophenyl)-6-hydroxy-benzothiazole (referred to as Pittsburgh compound B or PIB), a derivative of thioflavin T, labels plaques and cerebral amyloid angiopathy (CAA) in tissue sections from AD patients (6, 10, 11). The compound also crosses the blood–brain barrier (BBB), allowing peripheral administration of the amyloid-targeting reagent. This compound is readily labeled with carbon-11 for positron emission tomography (PET) scanning (10). Because the half-life of carbon-11 is $\approx$20 min, successful imaging will depend on very rapid brain entry, rapid brain clearance of nonspecifically bound and free tracer, and specific, prolonged binding of the tracer to amyloid-β targets. Therefore, we sought to characterize the kinetics of brain entry, plaque binding, and brain egress by means of direct, real-time imaging in transgenic mice that develop senile plaques as they age. We capitalized on the fluorescent properties of the compound and used our multiphoton microscopy techniques to image PIB in the brains of living transgenic mouse models of AD. By inserting an i.v. line into a mouse, timed injections of fluorescent compound were administered while imaging a volume of the brain over time. This four-dimensional imaging results in real-time detection of the appearance of PIB in vessels, crossing the BBB, labeling amyloid deposits, and clearing from the brain. The results demonstrate that PIB is ideally suited for detecting amyloid deposits *in vivo* in transgenic mice, and this finding should translate directly to successful imaging in humans.

Methods

PDAPP (12) (18–20 months old), Tg2576 (13) (18–20 months old), and PS-APP (14) (12 months old) mice were used for these experiments. Mice were anesthetized with Avertin and prepared surgically for cranial imaging, as described (6, 8). At least $n = 3$ mice were used for each injected compound. An i.v. line was placed in a tail vein of the animal and glued into place (cyanoacrylate adhesive, Krazyglue) for stability. Measured doses of fluorescent compounds (0.1–10 mg/kg) were delivered at time 0 by bolus injection during image acquisition. All compounds (PIB, thioflavin T, and thioflavin S) were dissolved in 20% DMSO, 80% propylene glycol solution. Multiphoton fluorescence excitation was accomplished with 750-nm light from a mode-locked, Ti:Saphire laser (Tsunami, Spectra-Physics). Fluorescence emission was collected by using a photomultiplier tube (Hamamatsu, Ichinocho, Japan) and an interference filter centered at 440 nm (Chroma, Technology, Brattleboro, VT). A Bio-Rad multiphoton microscope was used for imaging, mounted on an Olympus BX50WI upright microscope. A $\times$20 water immersion objective (0.45 numerical aperture, Olympus) was used for acquisition. 3D volumes comprising 615 $\times$ 615 $\times$ 150 μm were acquired sequentially, resulting in four-dimensional movies of a volume of the brain over time with a temporal resolution of 30 sec. In some cases, 615 $\times$ 615 $\times$ 35-μm volumes were acquired with a temporal resolution of 8 sec. Vascular amyloid was defined as rings of amyloid surrounding meningeal vessels, whereas plaques were defined as morphologically distinct deposits deeper within the parenchyma. Thioflavin S staining was used to label both types of amyloid deposition definitively. PIB staining was identical to thioflavin S staining in

This paper was submitted directly (Track II) to the PNAS office.

Abbreviations: AD, Alzheimer's disease; PIB, Pittsburgh compound B; CAA, cerebral amyloid angiopathy; BBB, blood–brain barrier; PET, positron emission tomography; ROI, region of interest.

†To whom correspondence should be addressed. E-mail: bbacskai@partners.org.

www.pnas.org/cgi/doi/10.1073/pnas.2034101100

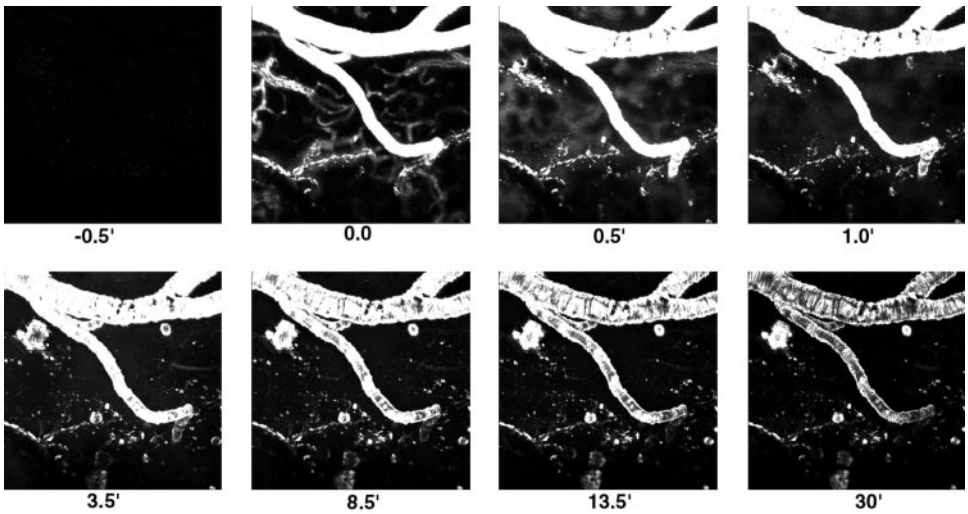

Fig. 1. Real-time imaging of fluorescent PIB crossing the BBB, labeling amyloid-β deposits, and clearing from the brain. Each frame is a maximum intensity projection of the fluorescence within a 3D volume of the brain of a live, transgenic, Tg2576 mouse, acquired with a multiphoton microscope. Each 3D volume required 30 sec to obtain. Each frame is 615 $\times$ 615 μm wide and $\approx$150 μm deep. A bolus i.v. injection of 2 mg/kg PIB was made shortly before $t = 0$ min. PIB is fluorescent, allowing monitoring of its entry into brain (across the BBB), binding to amyloid plaques and CAA, and clearance from brain. Note that brain entry is very rapid (within 30 sec), amyloid targeting occurs within 1 min, and clearance of unbound fluorescence occurs within several minutes. Plaques and CAA are labeled completely within 20 min and remain labeled for the full 30 min.

mouse tissue and human AD tissue. Diffuse amyloid deposits were not detected with PIB or thioflavin S. A maximum intensity projection of each volume was created for each time point and analyzed by defining regions of interest (ROIs) and measuring the intensity of fluorescence over time within vessels, plaques, and parenchyma by using Scion IMAGE (Scion, Frederick, MD) software. For histochemical analysis, animals were killed, and the brains were removed, fixed in 4% paraformaldehyde for 24 h, and cryopreserved in a 15% glycerol solution. Tissue sections (40 μm thick) were cut with a freezing sledge microtome and imaged with multiphoton microscopy. Pictures of plaques fluorescently labeled with PIB throughout the coronal sections of brain were obtained by using identical imaging conditions described for *in vivo* microscopy. The tissue sections were then incubated in 0.01% thiazine red R in PBS for 20 min at room temperature. This histochemical stain, like thioflavin S, labels dense-core plaques and CAA, but emits red fluorescence (550 nm), which can be readily distinguished from PIB. The tissue sections were reimaged with two-channel detection.

Results

This article takes advantage of the intrinsic fluorescence of PIB and the light microscopic imaging approach, multiphoton microscopy, for *in vivo* imaging in transgenic mouse models of AD (15, 16). We prepared 18- to 20-month-old Tg2576 (13) or PDAPP (12) mice for brain imaging by replacing a section of skull with an 8-mm round coverslip, permanently attached with bone cement (6). An i.v. line was implanted into a tail vein, and the anesthetized animal was placed on the stage of a multiphoton microscope (1024ES, Bio-Rad). 3D volumes of the brain were imaged by acquiring 2D images at progressively deeper planes of focus, up to 150 μm deep from the surface. The 3D volumes required 30 sec for acquisition and were collected continuously for up to 1 h. For higher temporal resolution collection, 8-s volumes (35 μm deep) were acquired. As shown in Fig. 1, autofluorescence was barely detectable in the untreated 20-month-old Tg2576 animal at $t = -0.5$ min; however, bright fluorescence appeared almost immediately after a bolus i.v. injection of 2 mg/kg PIB (in 80% propylene glycol/20% DMSO). The fluorescence first appeared in large and small blood vessels within the brain. Within 30 sec, the smallest, capillary-sized vessels appeared larger in diameter and less clearly distinguished, as the fluorescent dye crossed the BBB and entered the parenchyma. Larger vessels, which are not a site for diffusion from blood to brain, remained sharply outlined. Within 1 min, the brain parenchyma was nearly uniformly bright in fluorescence, and amyloid-β deposits were partially labeled. Amyloid angiopathy was the first to be labeled, followed by parenchymal dense-core plaques, which were first labeled at their periphery, and gradually filled in to the core. Diffuse amyloid deposits were not detectable, because PIB binding matched thioflavin S staining. Complete labeling of amyloid angiopathy occurred within 1 min; labeling of plaques peaked at $\approx$20 min. The majority of the residual fluorescence was cleared from the brain and blood vessels within 15 min. A movie of this experiment is shown in Movie 1, which is published as supporting information on the PNAS web site, www.pnas.org.

Fluorescence remained associated with the amyloid deposits at 1 h after injection. In separate experiments, PIB-labeled amyloid-β deposits were detectable up to 3 days after a single i.v. injection (data not shown). Plaque labeling could also be readily detected 24 h after i.p. injection of 10 mg/kg PIB. Fig. 2*A* shows a quantitative analysis of the kinetics of PIB distributions in the Tg2576 mouse. This graph illustrates the rapid appearance of fluorescent dye in blood vessels, the immediate and subsequent entry into the parenchyma across the BBB, and the relatively fast decay of fluorescence from the circulation and the parenchyma. Labeling of vascular amyloid was almost immediate and was sustained, whereas parenchymal Aβ deposits took slightly longer to label completely, but then remained stained. Fluorescence from entire plaques was measured, so that the 15-min lag period seen in Fig. 2*A* before the intensity of plaque fluorescence matches that of cerebrovascular amyloid most likely reflects the increase in labeling from the periphery to the core of the plaques. Some diffuse fluorescence remained in the circulation and the parenchyma, but remained a small fraction of the initial blush of compound. Therefore, these results demonstrate, in real time, that PIB enters the CNS rapidly, targets amyloid-β deposits specifically, and is cleared from the brain quickly when not bound to amyloid.

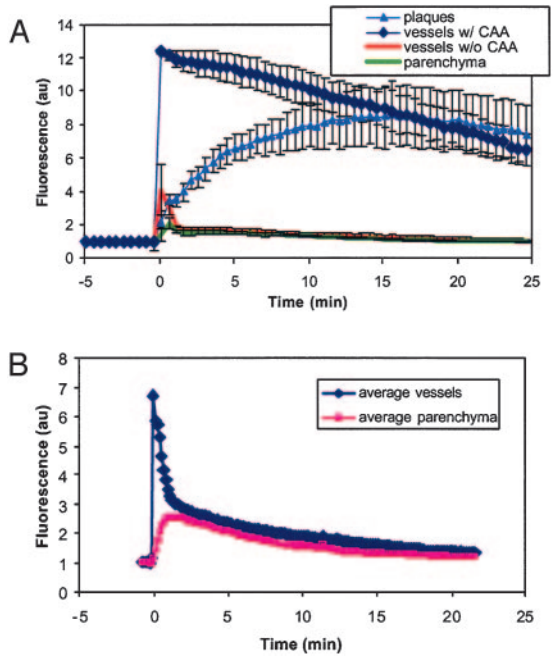

Fig. 2. Time course of PIB kinetics in Tg2576 mouse brain and cerebral vasculature at the level of single plaques and vessels. (*A*) These traces are averages from at least three ROIs from the image data shown in Fig. 1. ROIs were drawn within blood vessels containing CAA (◆) or without CAA (●), plaques (▲) or within the parenchyma (□). For each time point in the experiment, a maximum intensity projection was made of the imaging volume, which was a 615 × 615 × 150-μm deep cortical volume. The mean fluorescence intensity from within each ROI was calculated for each time point, and the average of the ROIs were plotted versus time, for up to 30 min. An i.v. injection of 2 mg/kg of the fluorescent compound PIB was made at t = 0 min. The fluorescence showed up almost immediately in the blood vessels, labeling CAA rapidly. The compound crossed the BBB quickly, entered the parenchyma, and labeled parenchymal amyloid-β deposits (plaques). Complete labeling of plaques was not immediate, because the outer fringes of plaques were labeled first, followed by gradual filling of the cores. Rapid clearance of fluorescent compound occurred in blood vessels without CAA and parenchyma. These kinetics of PIB entry into brain, labeling of amyloid-β deposits, and rapid clearance of unbound tracer demonstrate the utility of this compound for radiolabeled imaging experiments. (*B*) PIB time courses in WT C57/BL/J6 mice are plotted. These traces are averages from at least three ROIs. The traces are the average of the ROIs from two mice, imaged identically. These animals did not develop CAA or parenchymal amyloid-β deposits. ROIs were drawn within blood vessels (◆) or within the parenchyma (■). For each time point in the experiment, a maximum intensity projection was made of the 615 × 615 × 35-μm imaging volume. The mean fluorescence intensity from within each ROI was calculated for each time point, and the average of the ROIs were plotted versus time, for up to 30 min. An i.v. injection of 2 mg/kg of the fluorescent compound PIB was made just before t = 0 min. The fluorescence developed almost immediately in the blood vessels and dissipated rapidly. The compound appeared in the parenchyma with a short delay and was then cleared over time. No structures within the brain were labeled in these mice.

As a test of whether PIB access to neuropil depended on the presence of specific pathological changes or the mutant APP transgene, we examined a series of WT mice. In 3-month-old C57/BL/J6 mice, the kinetics of brain entry of the compound was similar, but no specific labeling with PIB was observed. Fig. 2*B* demonstrates the kinetics of brain entry after i.v. injection of the compound. As in transgenic mice, the dye appeared rapidly in the circulation, crossed the BBB quickly, and was then cleared quickly. Barely detectable amounts of fluorescence remained in the circulation and the parenchyma after 30 min, but no labeled structures were evident (data not shown).

Results similar to those obtained in the Tg2576 mice were obtained in 18- to 20-month-old PDAPP mouse brain, an alternative mouse model of amyloid-β deposition expressing a different mutant human APP transgene (12). As shown in Fig. 3, there were fewer, smaller dense-core plaques, but despite these differences the plaques were labeled with kinetics similar to those in the Tg2576 mouse. These data are shown in Movie 2, which is published as supporting information on the PNAS web site. Because at this age PDAPP mice have considerably less CAA than Tg2576 mice, this result also argues against a CAA-related breakdown in BBB as being responsible for access of PIB to the neuropil. In this experiment, 10 mg/kg PIB was injected at time 0 and resulted in the prolonged detection of circulating fluorescence. We were also able to obtain similar high-contrast fluorescent images of amyloid deposits at much lower doses of injected reagent (<0.15 mg/kg); however, circulating fluorescence was difficult to detect at these concentrations, precluding after the kinetics of brain entry and egress. The tracer levels of compound used for PET imaging in humans are on the order of 0.0001 mg/kg, far less than the doses used here for fluorescence imaging. All together, our analysis indicates that PIB labels Aβ deposits in different transgenic mouse models of AD, in different strains of mice, with different transgenes. Thus, the labeling is not specific to one model of the disease.

To evaluate the specific ability of PIB to cross the BBB, we tested the parent compound of this derivative, thioflavin T, in living transgenic mice. Thioflavin T is not expected to efficiently cross the intact BBB because of its positive charge and low lipophilicity (6, 11, 17). We injected thioflavin T (2 mg/kg) into 20-month-old Tg2576 mice, capitalizing on its intrinsic fluorescence, which is detectable with multiphoton microscopy. The compound rapidly appeared in the circulation after i.v. injection, but did not appear to enter the parenchyma. Vascular amyloid deposits, however, were weakly labeled with this approach, indicating that this pathology was accessible from the lumen of vessels or that some thioflavin T was able to cross the BBB (Fig. 4*A*). Vessels remained fluorescent (fluorescent angiography) for the duration of image acquisition (30 min after injection). After recording the time course of thioflavin T injection, the animal was killed, the cranial window on the mouse was removed, and thioflavin T (0.01% in PBS) was added directly to the surface of the brain for 20 min. A new coverslip was applied, and the same volume of brain was reimaged. At this point, the labeled amyloid angiopathy was easily reimaged, but appeared brighter, and parenchymal senile plaques were now also labeled (Fig. 4*B*). This result indicates that if thioflavin T crossed the BBB it was of insufficient amounts to label parenchymal Aβ deposits. The fluorescence from within the cerebral vessels was no longer detectable, because of the postmortem breakdown of the BBB. In parallel experiments, direct application of thioflavin T to the cortex of mice or sections of brain tissue labeled CAA and compact plaques, demonstrating that the failure of thioflavin T to label plaques after i.v. injection is related to its poor BBB permeability.

Interestingly, when thioflavin S was injected i.v. into a transgenic mouse, it was unable to label either parenchymal Aβ deposits or vascular amyloid deposits. Subsequent topical application of thioflavin S showed that both vascular and parenchymal Aβ deposits were present in these animals and could be labeled by direct application of the dye (data not shown). Thioflavin S is a poorly defined mixture of at least six compounds (18). Thioflavin S itself is thought to contain both positive (two quaternary benzothiazolium nitrogens) and negative charges (one sulfonic acid). In addition, thioflavin S (molecular weight = 512) is considerably larger than thioflavin T (molecular weight = 284). Both of these properties would be expected to limit the brain entry of thioflavin S to minimal levels. This result dem-

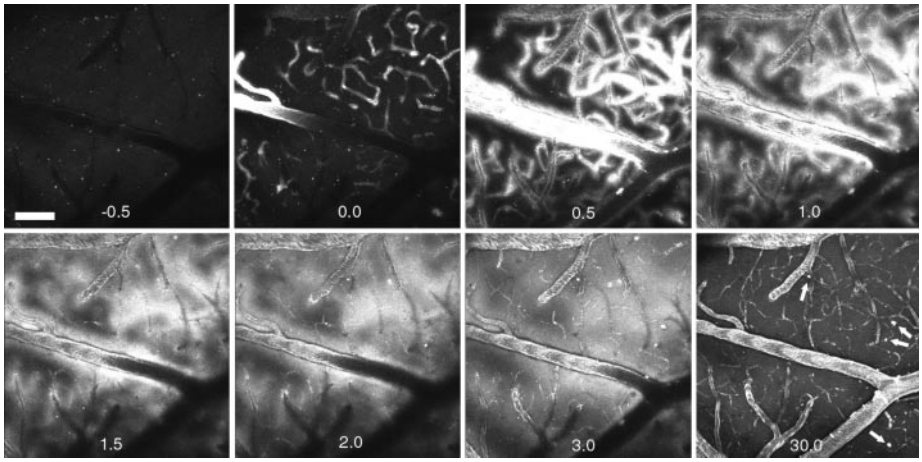

Fig. 3. PIB kinetics in a PDAPP mouse model. Each frame is a maximum intensity projection of the fluorescence within a 3D volume of the brain of a live, transgenic PDAPP mouse, acquired with a Bio-Rad multiphoton microscope. Each 3D volume required 30 sec to obtain. Each frame is 615 × 615 μm wide and ≈150 μm deep. An i.v. injection of 10 mg/kg PIB was made just before $t = 0$ min. Note that the fluorescent compound appears within blood vessels almost immediately. At $t = 0.5$ min, the vessels appear larger in diameter and ''fuzzy'' as the compound crosses the BBB and enters the parenchyma. This is seen in the next time points, $t = 1$ and 1.5 min. Within 3 min, parenchymal plaques are labeled and remain labeled at $t = 30$ min (arrows). This transgenic animal had few and small parenchymal plaques and little CAA. The CAA was labeled within 0.5 min and remained labeled for >30 min. By 30 min, the diffuse fluorescence of the blood vessels and parenchyma was markedly reduced compared with the maximal brightness achieved at $t = 1$–3 min. Some nonspecific fluorescence remains, probably caused by the large dose of PIB given in this animal. (Scale bar: 100 μm.)

onstrates that vascular amyloid is not accessible from the lumen of blood vessels, and, therefore, thioflavin T can penetrate the BBB more readily than thioflavin S. It is interesting that this slight permeability of thioflavin T may make it an ideal agent for selectively labeling CAA in the presence of parenchymal plaque amyloid, even when the latter is much more abundant, as is typically the case in AD.

To demonstrate that PIB labels the appropriate population of amyloid deposits specifically, animals were injected with the compound peripherally, killed, and then counterstained with a known amyloid binding dye, thiazine red R. This compound leads to the same staining in tissue sections as thioflavin S, namely CAA, dense-core senile plaques, and neurofibrillary tangles. Thiazine red R has a red-shifted emission spectrum, allowing us to demonstrate colocalization of both PIB and thiazine red R. Fig. 5 illustrates the one-to-one matching of PIB after peripheral injection and thiazine red R fluorescence. Fig. 5*A* demonstrates that PIB labels amyloid deposits with very high contrast and does not bind to white matter. PIB does not label structures that are not also labeled with thiazine red R, and thiazine red R does not label structures that are not labeled with PIB. Fig. 5 is a representative tissue section from one of $n = 3$ transgenic mice. Therefore, peripherally injected PIB is highly specific for the pathological amyloid deposits found in the brains of these transgenic mouse models.

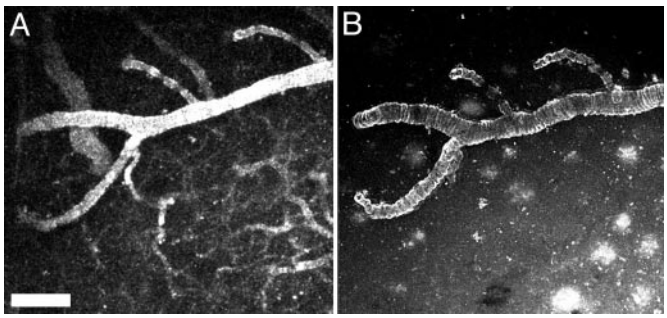

Fig. 4. Peripheral injection of thioflavin T labels CAA, but not parenchymal plaques in Tg2576 mice. Eighteen- to 20-month-old transgenic mice were injected with 2 mg/kg thioflavin T in 20% DMSO/80% propylene glycol i.v. Fluorescence was detected with multiphoton microscopy in the living mice, appeared almost instantaneously in the circulation, and remained there for up to 30 min. (*A*) A maximum intensity projection of a volume of the brain measuring 615 × 615 × 150 μm 10 min after injection. Fluorescence is present in all vessels (fluorescent angiography) and labels CAA to some extent in the large horizontal vessel in this image. Thirty minutes after imaging, the animal was killed, the cranial window was removed, and thioflavin T (0.01% in PBS) was applied directly to the surface of the cortex for 20 min. (*B*) The same volume (615 × 615 × 150 μm) of brain was reimaged, revealing high-contrast labeling of CAA as in *A* but without the luminal fluorescence. Numerous parenchymal amyloid-β deposits are now labeled within this volume. These results indicate that thioflavin T has some access to CAA, but does not cross the BBB effectively enough to label parenchymal plaques. (Scale bar: 20 μm.)

Discussion

The study and treatment of AD is plagued by the inability to definitively diagnose the disease in living human patients. A specific and reliable biomarker would greatly advance AD research, leading to a more complete understanding of the dynamics of the progression of the disease and providing the ideal quantitative end point for evaluating therapeutics aimed at removing the pathological lesions hypothesized to cause the disease. This article describes real-time imaging to characterize the suitability of a contrast agent that could allow direct detection of Alzheimer's amyloid in the brains of humans, when suitably radiolabeled for PET. The current studies capitalize on the fluorescent properties of the compound PIB, which is a novel derivative of thioflavin T that is able to cross the BBB and label amyloid deposits specifically (6, 10, 11). We demonstrate in living transgenic mice that develop amyloid plaques and CAA as they age, that the contrast agent rapidly crosses the BBB (within seconds) and labels these pathological lesions (within minutes). Unbound PIB is largely cleared from the parenchyma, and bound dye remains associated with amyloid deposits for several days. These results indicate that PIB rapidly and effectively targets the amyloid deposits that develop in three different transgenic mouse models. Thioflavin S and the parent compound thioflavin T are either

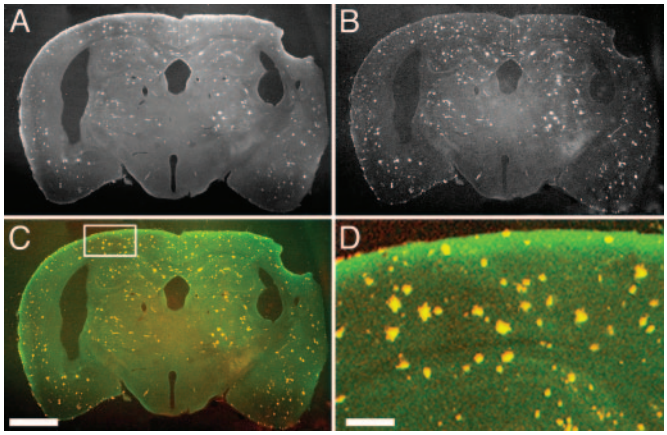

Fig. 5. Peripherally administered PIB labels plaques and CAA specifically in transgenic mice. Twelve-month-old PS-APP (3) mice were injected with 2–10 mg/kg PIB in 20% DMSO/80% propylene glycol i.v. The mice were killed 2 h after injection. The brains were removed and fixed in 4% paraformaldehyde for 24 h and cryopreserved in a 15% glycerol solution. Tissue sections (40 μm thick) were cut with a freezing sledge microtome, mounted onto slides without coverslips, and imaged with multiphoton microscopy. The sections were not washed or treated with any organic solvents. Pictures of plaques fluorescently labeled with PIB throughout the coronal sections of brain were obtained by using identical imaging conditions described for *in vivo* microscopy, but using a ×2 macro objective (numerical aperture = 0.14, Olympus). The tissue sections were then incubated in 0.01% thiazine red R in PBS for 20 min at room temperature. This histochemical stain, like thioflavin S, labels dense-core plaques and CAA but emits red fluorescence (550 nm). The tissue sections were reimaged with two-channel detection. Plaques and CAA labeled with PIB are shown (*A*) and are pseudocolored green in *C*, whereas thiazine red R fluorescence is shown in *B* and pseudocolored red in *C*. Overlapping fluorescence is yellow. (*D*) A higher-magnification view of the field defined by the rectangle in *C*. Note that amyloid deposits are stained with very high contrast with PIB, there is no staining of white matter, and the double labeling with thiazine red R is detected 100% of the time. (Scale bars: *A–C*, 1 mm; *D*, 200 μm.)

unable to cross BBB or cross in insufficient amounts for suitable sensitivity. However, the properties of thioflavin T may make it useful for the selective labeling of CAA.

In the present context of evaluating a potential PET tracer for amyloid imaging, a great advantage of multiphoton microscopy is resolution ($\approx$1 μm) that is 1,000-fold greater than that achievable with PET ($\approx$1 mm). This offers a unique ability to demonstrate the specificity of PIB at the level of individual plaques and vessels. In addition, the kinetics of tracer-target interactions can be measured in a semiquantitative way at the single plaque and vessel level.

Using this *in vivo*, high-resolution molecular imaging technique, we could study the real-time kinetics of PIB entry and clearance in WT mice. We demonstrated that the dye rapidly enters and leaves the brain and that little nonspecific binding occurs. This finding is critical for successful implementation of radiolabeled versions of PIB. Because of the short half-lives of the radionuclides used for PET and single-photon emission computed tomography scanning (20 min to several hours), differentiation of target signal from background noise must be accomplished very quickly. The current studies aid in the characterization of the kinetics of labeling in transgenic mice after administration, which should lay the groundwork for applications in humans.

The sensitivity of plaque detection using PIB with multiphoton microscopy was very good. We observed high-contrast imaging of amyloid deposits at the highest doses we used (10 mg/kg) that improved with the lowest doses (0.15 mg/kg). The doses of PIB used for fluorescence detection are many orders of magnitude higher than those used for PET scanning, so we expect the sensitivity to improve further with that technique. Imaging PIB with multiphoton microscopy does not predict the sensitivity obtainable with PET, however, because multiphoton microscopy results in an all-or-none detection of individual plaques within a very small volume of brain, whereas PET imaging will result in an averaged intensity of amyloid binding at low spatial resolution, but throughout the brain. The sensitivity of PIB for detection of amyloid with PET scanning will need to be addressed independently.

The current results demonstrate the impressive specificity of PIB binding to amyloid deposits in transgenic mouse brain at a histological level *in vivo*. Likewise, tissue sections of the brains of animals treated with PIB revealed a one-to-one colocalization with an established histochemical indicator of amyloid deposits. "Dense-core" plaques and CAA were labeled specifically in the transgenic mice and remained labeled up to 3 days after a single peripheral injection of PIB. Background staining was negligible, even in white matter.

Additionally, this article demonstrates the real-time kinetics of brain entry and target labeling of a CNS-targeting PET imaging tracer. Using multiphoton microscopy, and taking advantage of the fluorescent properties of the PET ligand PIB, we were able to image its appearance, entry, and clearance from the brain. The specific targeting and kinetics of the binding site of the probe (amyloid-β) was also readily distinguishable, with histochemical precision. Other radio-imaging probes may be amenable to a similar kind of kinetic evaluation exploiting either intrinsic fluorescent properties or modifications to enable fluorescent detection.

In summary, the direct demonstration of the kinetics of brain entry and target labeling of the specific amyloid-targeting compound (PIB) indicates that the radiolabeled ligand will be suitable for use in targeting amyloid-β structures in human patients and may ultimately prove to have diagnostic utility.

We thank Drs. D. Games and D. Schenk (Elan Pharmaceuticals) for access to PDAPP mice. This work supported by National Institutes of Health Grants AG08487 (to B.T.H.), AG18402 (to C.A.M.), AG01039 (to W.E.K.), AG20226 (to W.E.K.), AG15453 (to B.T.H.), EB00768 (to B.J.B.), and AG020570 (to B.J.B.), an Alzheimer Association Pioneer Award (to B.T.H.), Alzheimer Association Grants IIRG-95-076 (to W.E.K.), TLL-01-3381 (to W.E.K.), and NIRG-00-2355 (to Y.W.), and Institute for the Study of Aging/American Federation for Aging Research Grant 210304 (to Y.W.).

1. Hyman, B. T. & Trojanowski, J. Q. (1997) *J. Neuropathol. Exp. Neurol.* **56,** 1095–1097.
2. Markesbery, W. R. (1997) *Neurobiol. Aging* **18,** S13–S19.
3. Klunk, W. E. (1998) *Neurobiol. Aging* **19,** 145–147.
4. Eckelman, W. C. (2002) *Nucl. Med. Biol.* **29,** 777–782.
5. Shoghi-Jadid, K., Small, G. W., Agdeppa, E. D., Kepe, V., Ercoli, L. M., Siddarth, P., Read, S., Satyamurthy, N., Petric, A., Huang, S. C. & Barrio, J. R. (2002) *Am. J. Geriatr. Psychiatry* **10,** 24–35.
6. Mathis, C. A., Bacskai, B. J., Kajdasz, S. T., McLellan, M. E., Frosch, M. P., Hyman, B. T., Holt, D. P., Wang, Y., Huang, G. F., Debnath, M. L. & Klunk, W. E. (2002) *Bioorg. Med. Chem. Lett.* **12,** 295–298.
7. Zhuang, Z. P., Kung, M. P., Hou, C., Plossl, K., Skovronsky, D., Gur, T. L., Trojanowski, J. Q., Lee, V. M. & Kung, H. F. (2001) *Nucl. Med. Biol.* **28,** 887–894.
8. Klunk, W. E., Bacskai, B. J., Mathis, C. A., Kajdasz, S. T., McLellan, M. E., Frosch, M. P., Debnath, M. L., Holt, D. P., Wang, Y. & Hyman, B. T. (2002) *J. Neuropathol. Exp. Neurol.* **61,** 797–805.
9. Bacskai, B. J., Klunk, W. E., Mathis, C. A. & Hyman, B. T. (2002) *J. Cereb. Blood Flow Metab.* **22,** 1035–1041.
10. Mathis, C. A., Wang, Y., Holt, D. P., Huang, G.-F., Debnath, M. L. & Klunk, W. E. (2003) *J. Med. Chem.* **46,** 2740–2754.
11. Klunk, W. E., Wang, Y., Huang, G. F., Debnath, M. L., Holt, D. P. & Mathis, C. A. (2001) *Life Sci.* **69,** 1471–1484.

12. Games, D., Adams, D., Alessandrini, R., Barbour, R., Berthelette, P., Blackwell, C., Carr, T., Clemens, J., Donaldson, T., Gillespie, F., *et al*. (1995) *Nature* **373,** 523–527.
13. Hsiao, K., Chapman, P., Nilsen, S., Eckman, C., Harigaya, Y., Younkin, S., Yang, F. & Cole, G. (1996) *Science* **274,** 99–102.
14. Holcomb, L., Gordon, M. N., McGowan, E., Yu, X., Benkovic, S., Jantzen, P., Wright, K., Saad, I., Mueller, R., Morgan, D., *et al*. (1998) *Nat. Med.* **4,** 97–100.
15. Bacskai, B. J., Kajdasz, S. T., Christie, R. H., Carter, C., Games, D., Seubert, P., Schenk, D. & Hyman, B. T. (2001) *Nat. Med.* **7,** 369–372.
16. Christie, R. H., Bacskai, B. J., Zipfel, W. R., Williams, R. M., Kajdasz, S. T., Webb, W. W. & Hyman, B. T. (2001) *J. Neurosci.* **21,** 858–864.
17. Klunk, W. E., Debnath, M. L. & Pettegrew, J. W. (1994) *Neurobiol. Aging* **15,** 691–698.
18. Kelenyi, G. (1967) *J. Histochem. Cytochem.* **15,** 172–180.